Ecological Engineering 127 (2019) 338–347

Contents lists available at ScienceDirect

Ecological Engineering

journal homepage: www.elsevier.com/locate/ecoleng

Piezocone penetrometer measurements in coastal Louisiana wetlands

Navid H. Jafari[a,*], Brian D. Harris[a], Jack A. Cadigan[a], Qin Chen[b,c]

[a] Dept. of Civil and Environmental Engineering, Louisiana State University, 3255 Patrick F. Taylor Hall, Baton Rouge, LA 70803, United States
[b] Dept. of Civil and Environmental Engineering, Northeastern University, Boston, MA 02115, United States
[c] Dept. of Marine and Environmental Sciences, Northeastern University, Boston, MA 02115, United States

ARTICLE INFO

Keywords:
Piezocone penetrometer
Shear strength
Vegetation
Roots
Permeability
Pore pressure

ABSTRACT

The importance of geotechnical properties and behavior of wetland soils is underscored by the many studies on wetland loss, e.g., marsh edge erosion, shallow subsidence, wetland collapse, and uprooting. This study provides an overview of using a modified piezocone penetrometer to rapidly evaluate marsh shear strength, porosity, and electrical conductivity over a range of ecological, geological, and hydrologic wetland conditions. Field campaigns were conducted in Terrebonne Bay near Cocodrie, Louisiana to evaluate the efficacy of the cone to characterize the shear strength and stratigraphy of salt marshes. Based on the field measurements, the test method was found to be repeatable and consistent with the ASTM D5778 standard guideline. The piezocone soundings were used to evaluate the shear strength and stratigraphy of the vegetation root mat, organic clay, and inorganic clay layers. These findings were synthesized into an idealized wetland geotechnical framework for developing mechanistic models of wetland loss.

1. Introduction

The importance of geotechnical properties and behavior of wetland soils is underscored by the many studies on wetland loss, e.g., marsh edge erosion, shallow subsidence, wetland collapse, and uprooting (Knutson, 1987; Pestrong, 1972; Redfield, 1972; Day et al., 2011). For instance, Howes et al. (2010) indicate that the shallower vegetation root mat in the low salinity wetlands in upper Breton Sound compared to the more saline lower Breton Sound contributed to the significantly more land erosion in upper Breton Sound during Hurricane Katrina. Moreover, the rate of erosion at the marsh edge is a key parameter for predicting the longevity of a given vegetated wetland, including future marsh creation projects and sediment diversions proposed in the Louisiana coastal protection and restoration master plan (CPRA, 2017). Marsh soil strength and vegetation community, or wetland type, along with hydrodynamic characteristics, control the rate-of-retreat at marsh edges (Allison et al., 2017). Sasser et al. (2018) demonstrate the positive relationship between belowground biomass and soil strength. In particular, soil erosion rates across salt marsh regions are found to be closely related with plant species diversity, plant cover, root biomass, soil texture, and carbon stock (Ford et al., 2016). However, existing prediction models for marsh stability and evolution (e.g., Schwimmer, 2001; Mariotti and Fagherazzi, 2010; Mariotti, 2010; Marani et al., 2011) predominantly focus on wave energy and lump soil and vegetation effects into empirical constants. Consequently, the existing capability of predicting marsh edge erosion rate as a function of wave power and soil and vegetation properties is rather limited. For instance, Allison et al. (2017) showed that without taking the marsh platform, soil, and vegetation into account, the relationships between marsh edge erosion rates and wave power on a basin or coastal-wide scale are not strong enough statistically to serve as a useful predictive model. More recent erosion models (e.g., Leonardi and Fagherazzi, 2015; Johnson, 2016; Bendoni et al., 2014, 2015) directly or indirectly incorporate the undrained shear strength of wetlands.

Characterizing the compressibility properties of wetlands is also critical to understanding the interlinked processes of sediment compaction due to burial and self-weight consolidation (i.e., leading to a rearrangement of the mineral skeleton) and organic loss as the result of biological and chemical decay (Allen, 2000; Brain et al., 2011, 2012; Brain, 2015). In another case, hydrologic modeling and field studies are investigating plant zonation and hydrologic variability, with an emphasis on spring-neap tidal cycles (Wilson et al., 2015; Xin et al., 2010; Wilson and Morris, 2012). In particular, Ursino et al. (2004) show the relevance of the unsaturated subsurface ground-water regime with respect to the growth of halophytic vegetation in areas cyclically subjected to tidal inundation, such as in the Venice lagoon salt marshes. As result, evaluating the shear strength, compressibility, and permeability of wetland soils is necessary to build high-fidelity numerical models and

* Corresponding author.
E-mail addresses: njafari@lsu.edu (N.H. Jafari), bharr96@lsu.edu (B.D. Harris), jcadig1@lsu.edu (J.A. Cadigan), q.chen@northeastern.edu (Q. Chen).

https://doi.org/10.1016/j.ecoleng.2018.12.012
Received 12 June 2018; Accepted 6 December 2018
Available online 12 December 2018
0925-8574/

theoretical frameworks for predicting the capacity of wetlands to withstand the impacts from storm surge and waves, erosion, subsidence, and hydrologic forcing.

Vegetation roots are known to affect soil strength, e.g., mechanical reinforcement derived from fine roots acting as tensile reinforcement (Gray and Sotir, 1996). Roots affect soil hydrology by reducing water content through evapotranspiration and increasing soil permeability (Collison et al., 1995; Gray and Sotir, 1996; Kim et al., 2013; Coops et al., 1996; Durocher, 1990; Meijer et al., 2015; Micheli and Kirchner, 2002; Pollen, 2007; Thorne, 1990; van Eerdt, 1985). Plant root mucilage, combined with wetting and drying cycles, affects soil structure generation in the rhizosphere soil around the roots (Pohl et al., 2009; Fattet et al., 2011). Environmental factors that alter wetland vegetation and soil platform include the vegetation species and root biomass (Turner, 2011; Sasser et al., 2018), surface compaction and corresponding soil strength increase caused by desiccation from drying and wetting cycles (Day et al., 2011), and discontinuities in the soil profile. For example, a lens of inorganic material deposited by a deliberate levee breach of the 1927 flood is suggested by Kearney et al. (2011) as a contributor to Louisiana wetland loss because this thin seam inhibited growth of abundant roots and rhizomes. As a result, wetland soils are notable for their physical and hydraulic heterogeneity, fine layering, and unique structural properties, e.g., root mat development. Because these soils are particularly difficult to sample in an undisturbed manner for laboratory experiments, in-situ test methods are necessary to characterize the stratigraphy and engineering behavior of wetlands.

Multiple geotechnical instruments have been used to measure the shear strength of marshes, including the field vane (Howes et al., 2010; Turner, 2011), miniature vane (Chen et al., 2013), torvane (Wilson et al., 2012), and mechanical cone penetrometer (Are et al., 2002). Meijer et al. (2015) proposed four different geometric shapes, i.e., blade, pull-up, pin vane, and corkscrew, based on geotechnical principles to quantify reinforced root resistance within a depth of 30 cm. Sasser et al. (2018) developed the wetland soil strength tester, which measures the combined torque resistance when inserting four 15 cm pins. The two instruments historically employed in coastal Louisiana wetlands to gauge shear strength profiles are the mechanical cone penetrometer and rotating vane apparatus (i.e., field-vane, miniature-vane, and torvane). The mechanical cone penetrometer provides measures of tip resistance and sleeve resistance continuously with depth (Are et al., 2002; Mullins, 2006; Day et al., 2011). Although the mechanical cone penetrometer provides a continuous profile of soil strength, electric piezocone penetrometers are now available that can also measure pore-water pressure, shear wave velocity, moisture content, and electrical resistivity (Robertson, 2009). However, the weight of the push frame and drive system of the penetrometer make it prohibitive for carrying in wetlands, thus applications in coastal marshes are limited. Furthermore, existing piezocones lack sensitivity in the tip resistance load cell because the typical resistance range is 0–50 MPa.

The field-vane apparatus measures the undrained shear strength at discrete intervals. The vane apparatus was designed for soft homogenous clay deposits and the results are typically used for designing earthworks and foundations (Terzaghi et al., 1996). The blade width for the field vane, miniature vane, and torvane are 65 mm, 16 mm, and 19 mm, respectively. In coastal marshes that contain roots and shell fragments, the vane shear strength can be artificially increased and inconsistent. Thus, a direct comparison of these instruments is difficult because they measure the response of different physical soil behavior, such as measuring soil strength by displacing soil at different depths, integrating over different areas (blade thicknesses), or in different directions (i.e., horizontal vs. vertical). In addition, soil strength in coastal marsh environments is expected to be typically more variable than other environments due to the abundance of soil biomass, pore water chemistry, organics, and widely varying grain-size distributions. This lack of a uniform assessment methodology creates uncertainty when comparing different investigations on marsh soils and adds complexity for attempting to draw broad conclusions from multiple sites across Louisiana, the U.S., and the world. Therefore, the objective of this study is to introduce a modified piezocone penetrometer that can rapidly evaluate marsh shear strength, porosity, and electrical conductivity over a range of ecological, geological, and hydrologic wetland conditions. Field campaigns were conducted in Terrebonne Bay near Cocodrie, Louisiana to evaluate the efficacy of the cone to characterize the shear strength and stratigraphy of salt marshes. A background of the cone penetrometer, test methodology, and spatial and depth integrated profiles are summarized and discussed herein with implications to sustainability of salt marshes.

2. Soil moisture and resistivity piezocone penetrometer

The piezocone penetrometer is routinely used in subsurface investigations to define the stratigraphy and engineering behavior for infrastructure projects (e.g., levees, bridges, landfills, residential housing and commercial development). The weight of the push frame and drive system of the penetrometer make it prohibitive for carrying in wetlands, thus applications in coastal marshes have been limited. To overcome the weight restrictions of the push frame and drive system, a new lightweight push frame was developed that is hand-operated and easy to maneuver through the wetlands. The push frame consists of an aluminum frame inserted into the ground to provide stability and verticality during penetration (Fig. 1). Because the cone is driven manually by the operators, the drive system consisting of a hydraulic jack is not

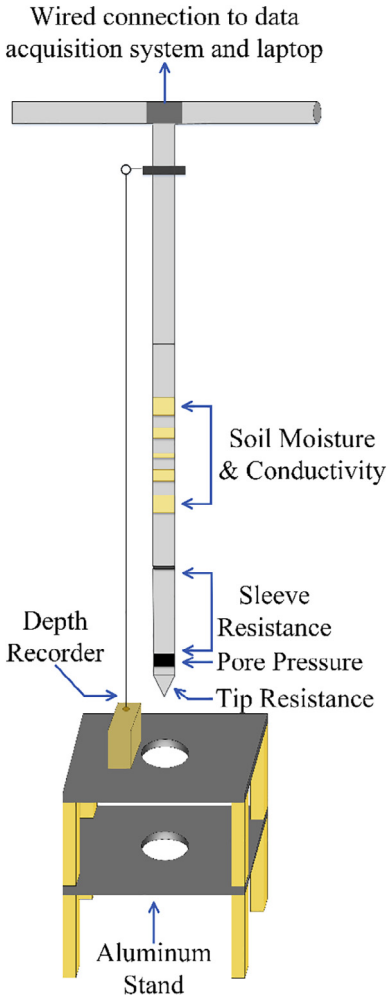

Fig. 1. Overview of the SMRT-CPTu and aluminum stand (schematic is not to scale).

needed. The major components and workflow of the cone test is shown in Fig. 1, which include the data acquisition system, cone penetrometer, and depth recorder.

The standard piezocone penetrometer measures tip resistance, sleeve friction, and pore-water pressure behind the conical tip in the u_2 position (Robertson, 2009). Various modules can be added onto the piezocone penetrometer for identifying contaminants, sampling, and obtaining seismic properties. For example, detecting changes in groundwater and soil chemistry is feasible by measuring changes in the electrical bulk resistivity or conductivity. Unsaturated soils and saturated soils with many non-aqueous-phase-liquid (NAPL) compounds exhibit high electrical resistivity (low conductivity). Dissolved inorganic compounds, such as those contained in brines and landfill leachates, can significantly decrease soil resistivity. Thus, the lateral and vertical extent of soil contamination can be evaluated via resistivity when the contaminate influences the electrical properties of the ground and/or groundwater. Penetrometers can also be outfitted with time domain reflectometry (TDR) or frequency domain reflectometry (FDR) probes to measure the dielectric constant of soil with depth. Dielectric constant is the ratio of permittivity of a material to that of a vacuum space (Antle, 1997) and is a function of soil porosity, volumetric moisture content, and the fractional bulk volume of each soil phase (i.e., solid, water, and gas). Dry soil has a dielectric constant K of 3–6, and adding water will increase the dielectric constant (dielectric constant of water is 80) (Topp et al., 1980). The presence of organic matter can also increase the dielectric constant due to the same reason (Vaz, 2003).

The piezocone penetrometer used herein incorporates both ecological parameters (Soil Moisture, Resistivity, and Temperature; SMRT) and geotechnical parameters (tip resistance, sleeve friction, and pore pressure; referred to as CPTu). Fig. 2(a) shows a diagram of the SMRT-CPTu and locations of each sensor. The soil resistivity is directly measured (No. 1 in Fig. 2a) by applying a voltage across the resistor bands. The resistivity (Ohm-m) is converted to electrical conductivity (microsiemens/m) by taking the reciprocal and then multiplying by 1,000,000. For example, 2 Ω-m equals to 500,000 mS/m. The soil moisture sensors (No. 2 in Fig. 2a) measure a frequency which can be correlated to volumetric moisture content using the universal equation proposed by Topp et al. (1980) or by calibrating the TDR probe for the specific soil to develop a soil specific moisture equation (Antle, 1997). The projected area of the conical tip in the standard CPTu is 10 cm^2 whereas the projected area of the SMRT-CPTu conical tip is 8 cm^2 because it was originally developed for agricultural applications. The tip resistance, sleeve friction, and pore pressure sensors for the SMRT-CPTu are rated for 22,500 kPa, 1000 kPa, and 3500 kPa. The uncertainty in the measurements is based on 0.2% of full-scale output. For example, the error in the tip resistance readings are ± 45 kPa, which is not sensitive enough for soft organic muck that is prevalent in coastal Louisiana because of the low undrained shear strengths (s_u < 10 kPa). As a result, a stainless-steel ball point tip attachment with a diameter 10.16 cm was fabricated to increase the projected area by a factor of 10 from the 8 cm^2 conical tip to 81 cm^2 (Fig. 2b). This results in one order of magnitude better precision in the tip resistance readings. However, it also prevents measurements of sleeve, pore pressure, resistivity, and soil moisture because the soil is pushed away by the ball point tip instead of flowing around the cone as occurs with the conical tip. Consequently, the ball point tip and conical tip need to be changed based on the required measurements. While this is a drawback, ongoing improvements to the cone workflow involve fabricating more sensitive load cells for the tip resistance.

To perform a cone sounding, the cone is inserted through two concentric opens in the aluminum frame. Prior to initiating the test, a baseline of tip resistance, sleeve friction, and pore pressure is recorded. This zeros out the load cells and is used in follow-up post-processing to monitor drift of the sensors. The depth recorder located on the aluminum frame is a potentiometer with a 1.8 m wire string. The string is pulled out usually 1.5 m or less and attached to a carabiner on the steel rod. As the cone is manually pushed into the marsh, the wire winds back into the potentiometer, which relays the depth of the cone readings to the data acquisition system. The tip resistance (q_c) and pore-water pressure (u_2) readings are used to determine the corrected tip resistance, $q_t = q_c + u_2 (1 - a)$, where a is cone area ratio (equal to 0.8). The undrained shear strength is determined as $s_u = (q_t - \sigma_v)/N_{kt}$, where the empirical factor N_{kt} is assumed 16 (Mesri and Huvaj, 2007). Because the ball point tip is utilized for evaluating shear strength, the u_2 shear induced pore-water pressures are not measured and the undrained shear strength is determined using only q_c tip resistance. To determine the ball point s_u, the q_c value is divided by the N_c factor, which is assumed 10 for soft organic soils (DeJong et al., 2011).

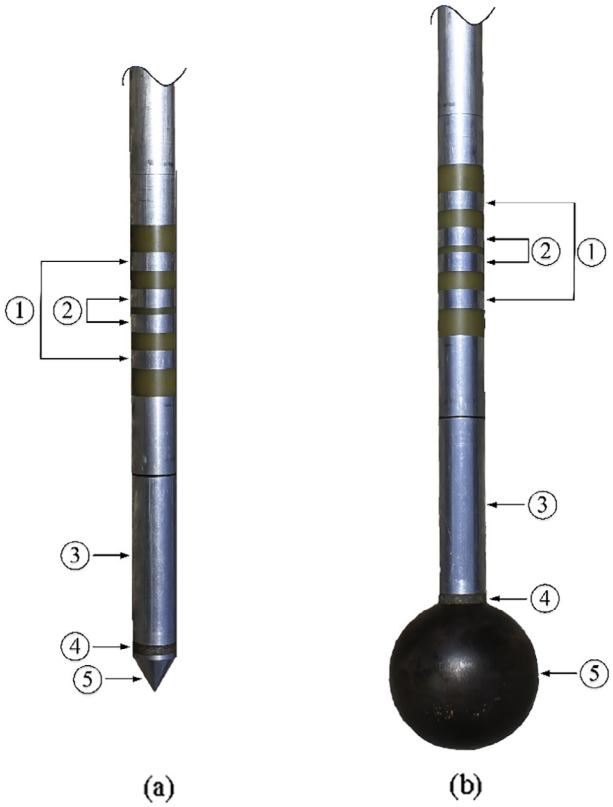

Fig. 2. Schematic of SMRT-CPTu: (a) conical tip, and (b) ball point tip. Stainless steel rings at (1) and (2) represent electrical conductivity and volumetric water content. Arrows (3), (4), and (5) point to sleeve friction, pore-water pressure element, and cone tip. The conical tip and CPT shaft diameter are 3.2 cm. The ball point tip diameter is 10.9 cm.

3. Site location

Terrebonne Bay near Cocodrie, LA was selected for the field testing because of the ease of access from Louisiana University Marine Consortium (LUMCON) and it is experiencing one of the largest wetland loss rates among Louisiana estuaries. During the period of 1932–2010, the Terrebonne Bay Basin lost 3080 km^2 (1190 mi^2), comprising of 25% of total wetland lost in coastal Louisiana (Couvillion et al., 2011). The dominant vegetation type is *Spartina alterniflora*, which is known for its extensive roots and below-ground rhizomes. Fig. 3 shows the specific locations of the CPTu soundings used to define the geotechnical and properties of the salt marsh. Approximately 130 cone penetrometer tests (combination of cone and ball tips) were conducted across three field expeditions (November 2016, April 2017, and November 2017). The November 2016 and 2017 campaigns were primarily focused on the marsh edge to determine the variation in geotechnical properties

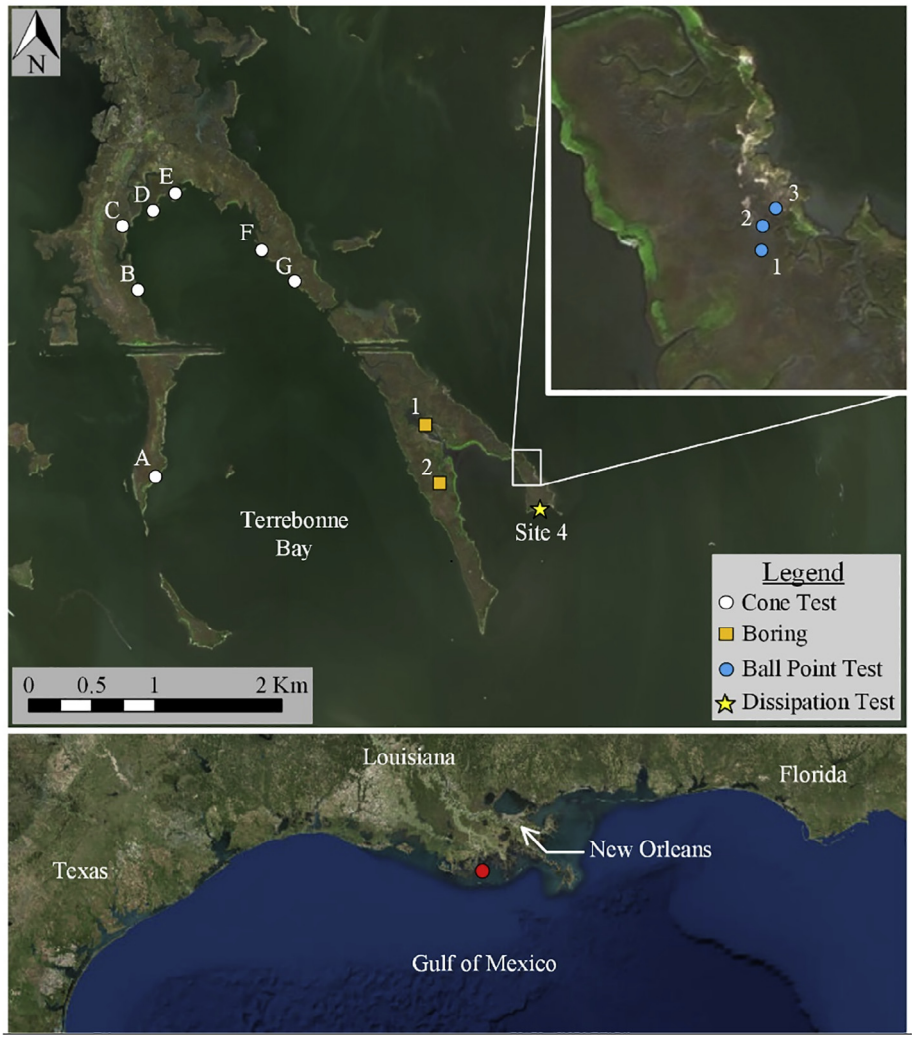

Fig. 3. Aerial view of the field site in Terrebonne Bay and CPT locations.

along long sections of shoreline (Sites A through G). The April 2017 field campaign focused on the interior of the wetlands (Sites 1–3). Two borings were retrieved at Sites 1 and 2, designated by the orange squares. The inset figure shows a cross-section of three ball points at Site 3. A pore pressure dissipation test was conducted at Site 4 to estimate the hydraulic conductivity of the organic soils.

4. SMRT-CPTu data analysis

Fig. 4 shows the tip resistance q_c for two CPTu soundings using the ball point tip. The data acquisition system initially recorded the cone output at 2 cm increments, i.e., total of 89 readings were collected for a 2.08 m sounding. After preliminary trials, the data system setting was changed to continuous readings to better capture the transition from the stiff vegetation root mat to the underlying organic rich soil. On average, the continuous readings provide twice as many readings when compared to the 2 cm increment option, thereby providing a higher spatial resolution. For example, the continuous readings in Fig. 4 show a smoother transition in tip resistance from the root mat to the underlying organic soil. Moreover, the continuous readings indicate when the cone penetration ceased in order for the operator to change the position of the wire string for the pontentiometer. The stop and start points are represented by a horizontal decrease and then increase in tip resistance when pushing was recommenced. An artificial increase in tip resistance is observed because of soil adhering to the ball tip, thus increasing the projected area and tip resistance when the cone is forced through the soil. After pushing a few centimeters into undisturbed soil, the adhered soil is removed and the tip resistance decreases. These affected points can be removed or reduced to follow the linear trend before the cone was stopped. In contrast to continuous readings, the depth-based option records measurements in a set increment so stoppages during the test are only detectable by a slight decrease in tip resistance. Furthermore, a vital aspect of the marsh resiliency lies within the strength of the vegetated mat so it is pertinent to quantify this accurately with depth. Within the first 0.5 m, the continuous and depth-based runs recorded 50 points and 16 points, respectively. Due to the sudden increase in push speed when punching through the vegetated mat, the depth-based test is not able to capture this layer at as high of a resolution when compared to the continuous setting. For both testing scenarios, the push speed neared 2 cm/s as per the ASTM standard (D5778) and was generally within the recommended range of 1–3 cm/s except between the depth of 0.75 m–1.25 m where it increased to about 5 cm/s (transition from vegetation to organic soil layers). As the manually pushed speeds in Fig. 4 are within the ASTM D5778 standard recommendations, it is possible to employ the technique and generate CPTu soundings between different regions and vegetation conditions.

Fig. 5 shows the repeatability of tip resistance and volumetric moisture content from the SMRT-CPTu tests alongside the interpreted wetland stratigraphy from soil cores and the cone readings. The results from Tests 1 and 2 show a stiffer vegetated mat consisting of higher volumetric water contents decreasing to a depth of 28 cm. Across the

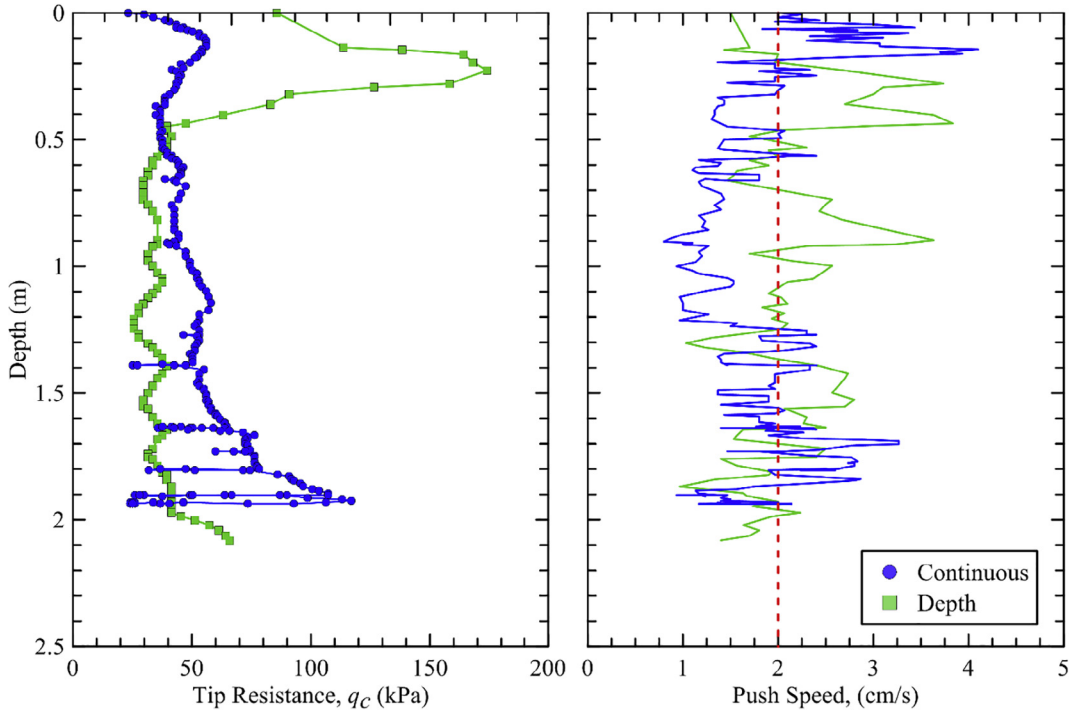

Fig. 4. Comparisons of continuous and depth-based recordings along with push speed for the SMRT-CPTu.

study area, the vegetated mat exhibited peak tip resistances and volumetric moisture content ranges of 60–100 kPa and 78–92%, respectively. The transition between the underlying organic clay with roots is indicated by a lower tip resistance that slightly increases with depth as well as a drastic drop in volumetric water content. The organic clay exhibited tip resistance and volumetric moisture content ranges of 30–60 kPa and 68–88%, respectively. The transition from the organic clay to the underlying interdistributary clay is indicated by a sharp increase in tip resistance alongside a decreasing volumetric moisture content. The CPT test extended only 0.5 m into this layer due to the lack of available reaction force.

Fig. 6 shows the combined geotechnical and ecological parameters obtained from the SMRT-CPTu. The tip resistance was obtained from the ball point tip, while sleeve friction, pore pressure response, volumetric moisture content, and soil electrical conductivity were measured using a conical tip. The sleeve friction can provide a trend of cohesion values with depth and can also be utilized to determine an approximate over consolidation ratio of the soils (Robertson, 2009). However, the sleeve friction in Fig. 6 does not register positive values except at the surface due to the reinforced roots and at depths of greater than 1.7 m.

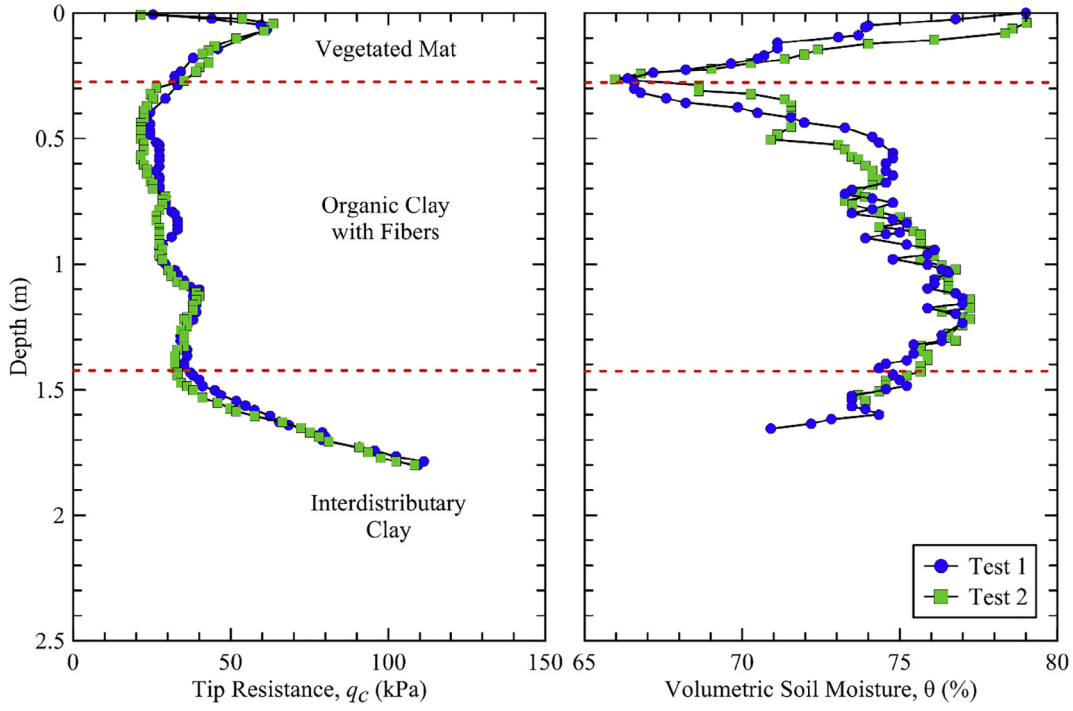

Fig. 5. CPT sounding to demonstrate repeatability and wetland stratigraphy, (a) tip resistance and (b) volumetric water content.

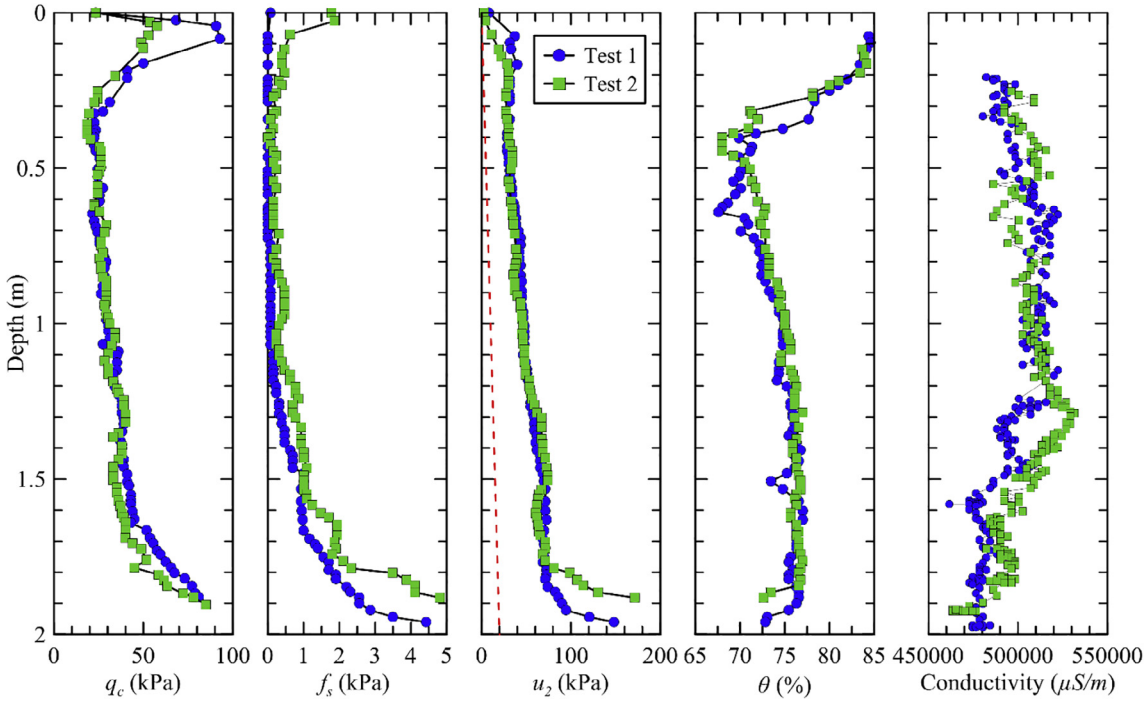

Fig. 6. Suite of geotechnical and ecological parameters obtained from SMRT-CPTu. (f_s = sleeve friction, u_2 = excess pore-water pressure, θ = volumetric water content, and electrical conductivity)

This same behavior is observed in the tip resistance, where the vegetation root mat causes a peak of 60 kPa and 100 kPa at 0.1 m before decreasing to a minimum of 20 kPa by 0.3 m. A slight linear increase in resistance is evident until a depth of 1.7 m, which indicates penetration into the inorganic clay layer. The pore-water pressure response is also linear with depth and greater than the hydrostatic line. This suggests that the organic clay is generating excess shear induced pore-water pressure during penetration. The pore pressure response increases when entering the inorganic interdistributary clay because the shear strength is higher and hydraulic conductivity is lower, thus the pore pressure cannot dissipate. In summary, the combination of tip and sleeve resistance along with pore pressure provide detailed information regarding the thickness of the root mat, shear strength of the organic clay, and lithology of the wetland platform. In addition to these findings, soil moisture and electrical conductivity can be used to determine porosity and bulk density and serve as a proxy for identifying saline soils. For saturated soils, porosity (n) and volumetric moisture content (θ) are equivalent because the volume of voids is completely filled with water ($n = \theta = w{\cdot}\rho_{dry}/\rho_w$). The average gravimetric water content (w) and dry bulk density (ρ_{dry}) obtained from cores of the organic clay layer are 150% and 1.3 g/cm^3, respectively. This leads to an average θ of 75% in the organic clay layer, which is consistent with the SMRT-CPTu sounding of 74%. The soil electrical conductivity in Fig. 6 remains constant with values approximately 500,000 μS/m, which is an order of magnitude lower than seawater (5,000,000 μS/m) but significantly higher than fresh water (5000 μS/m).

Fig. 7 shows profiles of ball point tip resistance and saturated bulk density (ρ_{sat}) obtained at Site 2 in Fig. 3. The bulk density was obtained from a 6 m core using the non-destructive Geotek multi-sensor core logger in order to verify the cone penetrometer profiles. For example, the variability and low bulk density in the upper 0.5 m of the core suggest the effects of vegetation roots. The bulk density becomes a constant value of 1.3 g/cm^3 from a depth of 0.5 m to 1.8 m, which is in agreement with nearly constant tip resistance and thus signifies the shear strength is also constant with depth for the organic clay layer. As the ball point tip increases in resistance at a depth of 2 m, the saturated bulk density increases from 1.3 g/cm^3 to 2 g/cm^3, confirming the transition from the organic clay to interdistributary clay layer. The saturated bulk density shows an inversely proportional relationship with volumetric water content which is especially true for high water content organic soils found in wetlands. This general relationship allows for a trend of saturated bulk density to be established from the volumetric moisture content readings from the SMRT-CPTu which is relevant to evaluate the soil composition in the wetland soils.

4.1. Spatially variability of tip resistance

Fig. 8 compares the variation of ball point tip resistance between *Spartina alterniflora* vegetated marsh at Site 1, 2, and 3 and an unvegetated mud flat (Boring 1 in Fig. 3). The vegetated test sites exhibited higher tip resistance near the surface to reflect the belowground biomass and identified the organic to interdistributary clay transition at 1.9 m. The peak resistance in the root mat occurs in Site 1, which is closer to the marsh edge, and generally decreases to Site 3 (interior marsh). This transition in tip resistance suggests that the root mass from the marsh edge to interior marsh is changing because of a combination of less sediment deposition, available nutrients, and hydroperiod (Day et al., 2011). In particular, the marsh edge is more aerated and surface elevation is higher than the interior marsh. This results in more inundation in the interior areas and anaerobic conditions that facilitate biogeochemical processes that reduce sulfate to hydrogen sulfide, thereby negatively impacting the belowground biomass and corresponding shear strength. This was evident from a qualitative perspective because walking on the marsh edge was feasible, but it became extremely difficult not to sink 0.5 m into the ground as the location of Site 3 was approached. The tip resistances within the organic clay increase from 30 kPa at 0.5 m to 80 kPa at a depth of 1.8 m. The slope of the tip resistance is approximately 38 kPa/m, which indicates a stiffer soil than measured tip resistances in Figs. 6 and 7. The spatial variability of tip resistance from Site 1 to Site 3, which are distanced about 20 m apart, is not present because the profiles overlap. In comparison to a vegetated marsh, the mudflat consisted of very soft soils such that the test was performed with the operator standing on the aluminum frame (Fig. 9). The tip resistance registered less than 20 kPa to a depth of 1 m

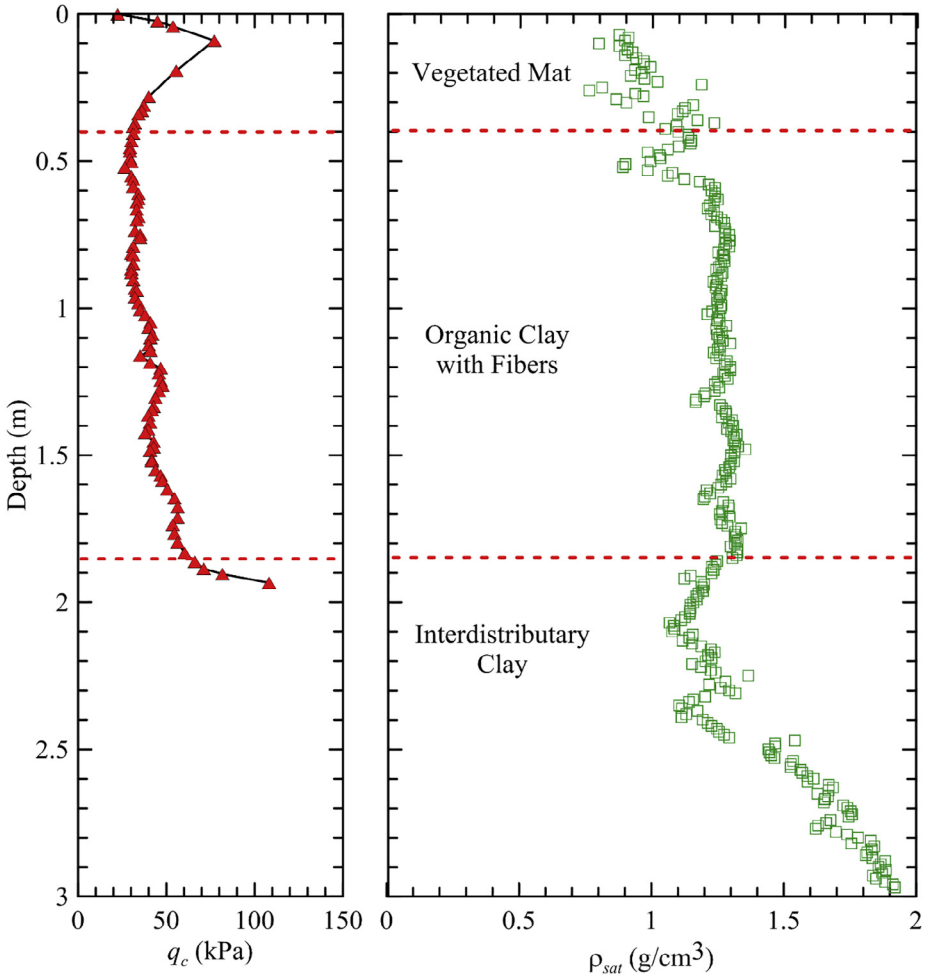

Fig. 7. Comparison between tip resistance and bulk density.

and the increased resistance at a depth of 2.2 m signifies a change in soil layering. The mudflat provides a baseline of organic soils and the subsequent changes to soil properties that can occur if a vegetation platform forms after a marsh restoration or sediment division project is constructed. As the continued wetland loss in Louisiana will result in new mudflats, a comparison of the soil properties at a fixed location before and after the vegetation platform is eroded can be also made with the SMRT-CPTu.

Fig. 10 shows the changes in tip resistance from Sites A to G (see Fig. 3). Across the 7 sites along the marsh edge, the vegetated mat thickness is similar (0.25 m) while the peak tip resistance ranged from 52 to 101 kPa in the vegetated root mat. In particular, Sites A, D, E, and G experienced the higher resistance values (~100 kPa) while Sites B, C, and F yielded lower resistance values (~65 kPa). The organic clay exhibited constant tip resistance with depth, ranging from 30 kPa to 60 kPa with an average of 38 kPa. This suggests that the magnitude of shear strength along the marsh edge is similar in this region. However, the piezocone soundings indicate that the depth to the interdistributary clay varies from Site A to G. In particular, the interdistributary clay was at a depth of 1.4 m at Site A and increased to ~2 m by Sites D and E. Moving from the interior of the bay towards the south, the depth to the inorganic clay decreases back to 1.6 m at Site G. While the shear strength of the organic clay does not vary, the thickness does vary by approximately 0.5 m. An implication of the thicker organic clay layer is that more compaction (assumed the same as consolidation) will occur, which will lead to lower surface elevations. If sediment deposition cannot keep pace with this compaction, the duration of the hydroperiod can increase beyond a healthy threshold (i.e., lowering vegetation biomass and strength). As a result, marsh edge erosion can accelerate due to lower vegetation strength when wind-generated waves directly impact the marsh scarp and lead to undercutting and marsh surface erosion near the edge.

4.2. Hydraulic conductivity of marsh soils

The measurement of hydraulic conductivity of marsh soils is an important parameter when focusing on surface-subsurface groundwater interactions, including nutrient and salinity gradients and the corresponding effect on the biogeochemical processes in the root zone. The SMRT-CPTu can estimate the in-situ hydraulic conductivity by performing a pore pressure dissipation test, which involves recording the decrease in excess shear-induced pore pressure values with time while the cone remains stationary. This test provides an indirect measurement of the hydraulic conductivity that is in agreement with laboratory results for organic clays (Jafari and Stark, 2017). Fig. 11 shows the results of a dissipation test conducted within the organic clay layer at Site 4 (see Fig. 3 for location). The SMRT-CPTu was pushed to a depth of 1.5 m below the ground surface and the excess pore pressure, generated by the insertion of the cone, was allowed to dissipate. The water table was assumed to be at the ground surface and the hydrostatic pressure was subtracted from the measured pore pressures. The test was terminated before 30 min was reached so a square root of time analysis was utilized to determine t_{50}, which signifies the time to reach 50% dissipation of the maximum excess pore pressure (Robertson and Cabal, 2015). The time to 50% pore pressure dissipation (~8.5 kPa) in Fig. 11 occurs at 143 s. The coefficient of consolidation (c_v) is estimated by

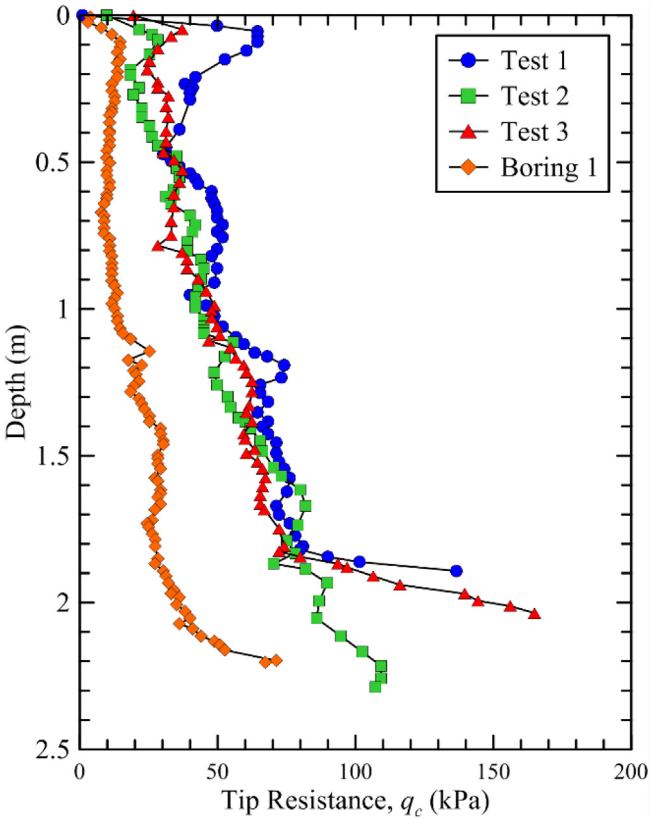

Fig. 8. Comparison of tip resistance of mud flat and *Spartina alterniflora* vegetated zone.

Fig. 9. Performing SMRT-CPTu sounding on a mudflat near Boring 1.

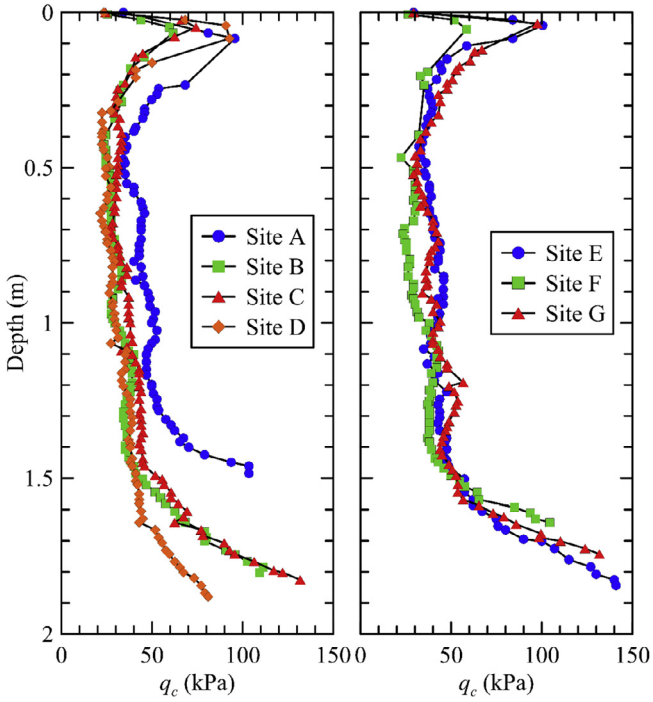

Fig. 10. Changes in tip resistance from Site A to G.

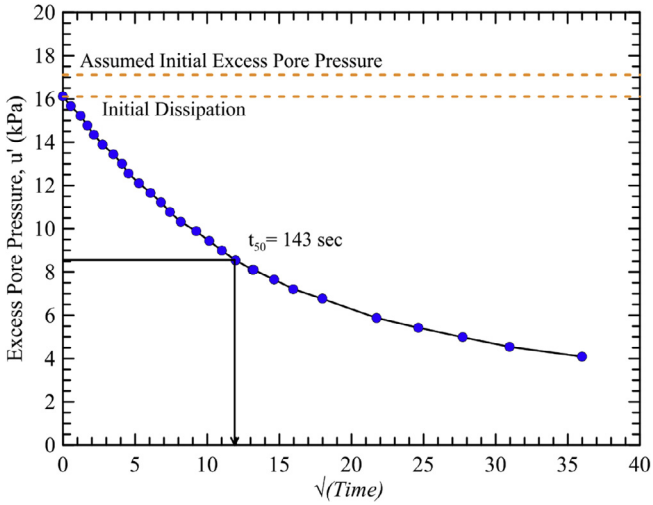

Fig. 11. Excess pore pressure dissipation of organic clay (time = seconds).

$c_v = (T_{50}/t_{50})r_o^2$, where T_{50} is theoretical time factor, t_{50} is the measured time for 50% dissipation, and r_o is the cone penetrometer radius (1.5875 cm). By assuming the coefficient of volume compressibility (m_v) of 1.4×10^{-3} kPa^{-1} for organic clays in coastal Louisiana (Jafari and Stark, 2017), the hydraulic conductivity (k_v) was estimated to be 4.8×10^{-7} cm/s using the relationship for c_v and rearranging to find $k_v = c_v \cdot m_v \cdot \gamma_w$, where γ_w is the unit weight of water (9.81 kN/m^3). Parez and Fauriel (1988) propose another empirical equation ($k_v = (2.51 \cdot t_{50})^{-1.25}$) to estimate the hydraulic conductivity k_v using only t_{50}. Applying this equation, the hydraulic conductivity k_v was estimated to be 2.0×10^{-6} cm/s, which is in agreement with the square root time method (Robertson and Cabal, 2015). The k_v of 2×10^{-6} cm/s suggests that flow through this layer is controlled by macropores (e.g., organic inclusions like roots, stems, fibers, bioturbation).

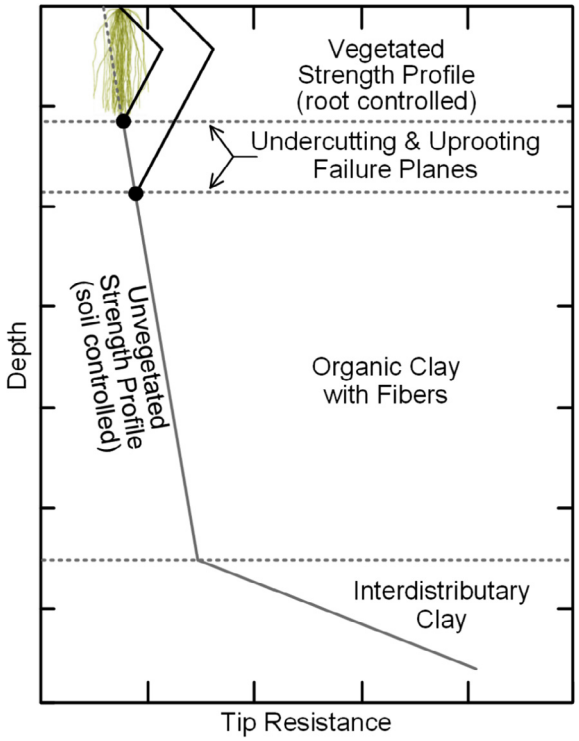

Fig. 12. Conceptual model of shear strength profile for coastal marshes (modified after Howes et al. (2010)).

4.3. Idealized wetland profile from CPTu soundings

The piezocone measurements and observations were synthesized into Fig. 12, which shows an idealized profile of shear strength versus depth to explain the mechanisms that can contribute to vulnerability of coastal marshes. Lower strengths occur at the marsh surface due to surficial sediments overlying the root system. As the cone penetrometer penetrates into the vegetation root mat, the peak strength is measured at depth before decreasing to a minimum at the organic clay layer interface, which is constant or slightly increasing with depth. The organic clay strength is anticipated not to change with time, but the abundance of belowground biomass can change the depth profile of vegetation strength. Belowground biomass production is seasonal so it is hypothesized that the vegetation root mat strength decreases during the winter. Belowground biomass can also change as a result of nutrients, salinity, hydroperiod, and vegetation type, which will be reflected in the strength profile. Similarly, if the wetland surface elevation is above the tidal regime, a desiccated surface results in higher strengths at the surface and a gradual transition to the normally consolidated soil. The interdistributary clay represents a stiffer normally consolidated foundation soil that is a result of increased overburden stresses.

The abrupt change in soil strength slope versus depth, especially at the interface of the root mat and organic clay, can result in failure planes or regions above which entire blocks of wetland soil can fail (Howes et al., 2010; Pizzuto, 1984; Thorne, 1990). In particular, hurricane storm surge and waves can apply sufficient shear stress to uproot and create a failure surface at the vegetation root mat interface with organic clay. For marsh edge retreat, wind-driven waves can lead to erosion through undercutting of the organic clay and surficial erosion of sediment at the surface and within the vegetative root mat. The latter mechanism results in erosion of the vegetation followed by the organic clay. When the root mat is stronger than the organic clay, undercutting is the driving mechanism of marsh edge erosion. The switching of mechanism behind marsh edge erosion is likely a function of seasonal variation of belowground biomass and cold front season. The thickness and shear strength of the organic clay can allude to the potential for shallow compaction, which can increase the hydroperiod of the marsh beyond a sustainable threshold. In summary, the shear strength and lithology of wetland platform can provide important information regarding the resiliency of the wetland to extreme events, environmental stressors, and long-term sea level rise.

5. Summary and conclusions

This study provides an overview of the importance of wetland soils for predicting wetland resilience and in-situ techniques to measure the geotechnical properties. A modified piezocone penetrometer was introduced to rapidly evaluate marsh shear strength, porosity, and electrical conductivity over a range of ecological, geological, and hydrologic wetland conditions. Field campaigns were conducted in Terrebonne Bay near Cocodrie, Louisiana to evaluate the efficacy of the cone to characterize the shear strength and stratigraphy of salt marshes. Based on the field measurements, the following conclusions are formed regarding the piezocone penetrometer, test methodology, and spatial and depth integrated profiles:

- Trials with the data acquisition elucidated that the continuous data recording option better captures the cone readings with depth, especially at the transition of vegetation root mat and organic clay where the push speed is significantly higher. The push speed of the piezocone tests varied with depth but were within the ASTM D5778 recommendation of 1–3 cm/s. Multiple cone soundings conducted at the same location also demonstrate the repeatability of the test method.
- The sleeve resistance, tip resistance, and volumetric water content provided the ability to capture the lithology of the wetland platform, from the vegetation root mat to the underlying organic clay and inorganic layers. The tip resistance of the vegetation root mat varied from the marsh edge to the interior wetland, indicating that ecological and hydrological conditions are spatially varying. The organic clay shear strength was typically in the range of 30–60 kPa and slightly increased with depth. The interdistributary clay consists of a higher strength due to the difficulty of penetrating through this layer. The mudflat resistance was less than 20 kPa. The saturated bulk density and porosity were compared to core data and show that the piezocone sounding can capture spatial trends and potentially serve as a proxy for organic matter content.
- The idealized profile of the wetland is a framework to start evaluating wetland loss by incorporating the geotechnical properties into the failure mechanism, including marsh surface erosion, root mat uprooting, undercutting of weaker organic clay, and shallow compaction of the organic clay layer. For example, the strength and depth of the root mat alludes to the potential for uprooting during an extreme event such as a hurricane. The thickness and strength of the organic clay provide an indication for shallow compaction and marsh edge erosion via undercutting, respectively. Forming mechanistic wetland loss models from this idealized profile will lead to better predictions for resiliency against future extreme events, environmental stressors, and long-term sea level change.

Acknowledgments

Support for this research was provided by the Louisiana Coastal Protection and Restoration Authority (CPRA) and administered by Louisiana Sea Grant (LSG) through its Coastal Science Assistantship Program (CSAP). The support by the USACE Coastal Hydraulics Laboratory Grant is greatly acknowledged. The authors appreciate the assistance of Jodie Crocker for her data analysis and manuscript preparation. Dr. Sam Bentley and Giancarlo Restreppo graciously provided the core data in Fig. 7. Professor Daniel Dias of Université Grenoble Alpes, France is credited in Fig. 9 performing the CPTu sounding and is

greatly thanked for his assistance in the April 2018 field campaign.

References

Allen, J.R.L., 2000. Morphodynamics of Holocene salt marshes: a review sketch from the Atlantic and Southern North Sea coasts of Europe. Quat. Sci. Rev. 19 (12), 1155–1231.

Allison, M., et al., 2017. Draft Coastal Master Plan. Coastal Protection and Restoration Authority, Baton Rouge, LA 2015, pp. 51.

American Society for Testing and Materials, 2012. D5778. ASTM International, West Conshohocken, PA.

Antle, C.L., 1997. Soil Moisture Determination by Frequency and Time Domain Techniques. Ohio University.

Are, D., et al., 2002. A portable, electrically-driven Dutch cone penetrometer for geotechnical measurements in soft estuarine sediments. J. Coast. Res. 18, 372–378.

Bendoni, M., et al., 2014. On salt marshes retreat: experiments and modeling toppling failures induced by wind waves. J. Geophys. Res. 119, 603–620.

Bendoni, M., et al., 2015. Process-based modelling of wave induced salt marsh edge erosion. In: IAHR World Congress, pp. 36.

Brain, M.J., et al., 2011. Compression behavior of minerogenic low energy intertidal sediments. Sediment. Geol. 233, 28–41.

Brain, M.J., et al., 2012. Modelling the effects of sediment compaction on salt marsh reconstructions of recent sea level rise. Earth Planet. Sci. Lett. 345–348, 180–193.

Brain, M.J., 2015. Compaction. In: Shennan, I., Long, A.J., Horton, B.P. (Eds.), Handbook of Sea-Level Research. Wiley, pp. 452–469.

Chen, Q., 2013. In: Sediment Transport: Monitoring, Modeling and Management. Nova Science Publishers, pp. 311–337 (Chap. 10).

Collison, A., et al., 1995. Impact of vegetation on slope stability in a humid tropical environment: a modelling approach. In: Proceedings of the Institution of Civil Engineers Water Maritime & Energy, pp. 168–175.

Coops, H., et al., 1996. Interactions between waves, bank erosion, and emergent vegetation: an experimental study in a wave tank. Aquat. Bot. 53, 187–198.

Couvillion, B.R., et al., 2011. USGS. National Wetlands Research Center, Lafayette, LA.

Day, J.W., et al., 2011. Vegetation death and rapid loss of surface elevation in two contrasting Mississippi Delta salt marshes: the role of sedimentation, autocompaction and sea-level rise. Ecol. Eng. 37, 229–240.

DeJong, J.T., et al., 2011. Evaluation of undrained shear strength using full-flow penetrometers. J. Geotech. Geoenviron. Eng. 137 (1), 14–26.

Durocher, M.G., 1990. Monitoring spatial variability of forest interception. Hydrol. Process. 4 (3), 215–229.

Fattet, M., et al., 2011. Effects of vegetation type on soil resistance to erosion: relationship between aggregate stability and shear strength. Fuel Energy Abstr. 87, 60–69.

Ford, H., et al., 2016. Soil stabilization linked to plant diversity and environmental context in coastal wetlands. J. Veg. Sci. 27, 259–268.

Gray, Donald H., Sotir, Robbin B., 1996. Biotechnical and Soil Bioengineering Slope Stabilization: A Practical Guide for Erosion Control. John Wiley & Sons, New York.

Howes, N.C., et al., 2010. Hurricane-induced failure of low salinity wetlands. PNAS 107, 14014–14019.

Jafari, N.H., Stark, T.D., 2017. Field scale hydraulic conductivity and compressibility of organic clays. Eng. Geol. 220, 52–64. https://doi.org/10.1016/j.enggeo.2017.01.015.

Johnson, C.L., 2016. Master's Thesis. Louisiana State Univ., Baton Rouge, LA.

Kearney, M.S., et al., 2011. Freshwater river diversions for marsh restoration in Louisiana: twenty-six years of changing vegetative cover and marsh area. Geophys. Res. Lett. 38 (L16405), 16. https://doi.org/10.1029/2011GL047847.

Kim, et al., 2013. Modeling the contribution of trees to shallow landslide development in a steep, forested watershed. Ecol. Eng. 61 (Part C), 658–668.

Knutson, P.L., 1987. In: The Ecology and Management of Wetlands. Timber Press, Portland, OR, pp. 161–175 (Chap. 13).

Leonardi, N., Fagherazzi, S., 2015. Effect of local variability in erosional resistance on large-scale morphodynamic response of salt marshes to wind waves and extreme events. Geophys. Res. Lett. 42, 5872–5879. https://doi.org/10.1002/2015GL064730.

Louisiana Coastal Protection and Restoration Authority, 2017. Louisiana's Comprehensive Master Plan for a Sustainable Coast.

Marani, M., D'Alpaos, A., Lanzoni, S., Santalucia, M., 2011. Understanding and predicting wave erosion of marsh edges. Geophys. Res. Lett. 38, L21401. https://doi.org/10.1029/2011GL048995.

Mariotti, G., 2010. Influence of storm surges and sea level on shallow tidal basin erosive processes. J. Geophys. Res.

Mariotti, G., Fagherazzi, S., 2010. A numerical model for the coupled long-term evolution of salt marshes and tidal flats. J. Geophys. Res. 115, F01004. https://doi.org/10.1029/2009JF001326.

Meijer, et al., 2015. New in-situ techniques for measuring the properties of root-reinforced soil – laboratory evaluation. Geotechnique.

Mesri, G., Huvaj, N., 2007. Shear Strength Mobilized in Undrained Failure of Soft Clay and Silt Deposits. Advances in Measurement and Modeling of Soil Behavior.

Micheli, E.R., Kirchner, J.W., 2002. Effects of wet meadow riparian vegetation on streambank erosion: 2. Measurements of vegetated bank strength and consequences for failure mechanics. Earth Surf. Proc. Landforms. 27, 687–697.

Mullins, G., 2006. In situ soil testing. The Foundation Engineering Handbook. Taylor & Francis Group.

Parez, L., Fauriel, R., 1988. Advantages from piezocone application to in-situ tests. Révue Française de Géotechnique 44, 13–27.

Pestrong, R., 1972. Tidal-flat sedimentation at Cooley Landing, Southwest San Francisco Bay. Sediment. Geol. 8, 251–288.

Pizzuto, J.E., 1984. Bank erodibility of shallow sandbed streams. Earth Surf. Process. Landforms 9 (2), 113–124.

Pohl, M., et al., 2009. Higher plant diversity enhances soil stability in disturbed alpine ecosystems. Plant Soil 324, 91–102.

Pollen, N., 2007. Temporal and spatial variability in root reinforcement of streambanks: accounting for soil shear strength and moisture. Catena 69, 197–205.

Redfield, A.C., 1972. Development of a New England salt marsh. Ecol. Monogr. 42, 201–237.

Robertson, P.K., 2009. Interpretation of cone penetration tests – a unified approach. Can. Geotech. J. 14, 465–481.

Robertson, P.K., Cabal, K.L., 2015. Guide to Cone Penetration Testing for Geotechnical Engineering. Gregg Drilling, sixth ed. .

Sasser, C.E., Evers-Hebert, E., Holm, G.O., et al., 2018. Relationships of marsh soil strength to belowground vegetation biomass in Louisiana coastal marshes. Wetlands 38, 401. https://doi.org/10.1007/s13157-017-0977-2.

Schwimmer, R.A., 2001. Rates and processes of marsh shoreline erosion in Rehoboth Bay, Delaware, U.S.A. J. Coast. Res. 17, 672–683.

Terzaghi, K., Peck, R.B., Mesri, G., 1996. Soil Mechanics in Engineering Practice. J. Wiley & Sons; Chapman & Hall, New York; London.

Thorne, C.R., 1990. Effects of vegetation on riverbank erosion and stability. In: Thornes, J.B. (Ed.), Vegetation and Erosion. Wiley, Chichester, pp. 125–143.

Topp, G.C., et al., 1980. Electromagnetic determination of soil water content: measurements in coaxial transmission lines. Water Resour. Res. 16, 574–582.

Turner, R.E., 2011. Beneath the salt marsh canopy: loss of soil strength with increasing nutrient loads. Estuar. Coasts 34. https://doi.org/10.1007/s12237- 010-9341-y.

Ursino, N., et al., 2004. Subsurface flow and vegetation patterns in tidal environments. Water Resour. Res. 40, W05115. https://doi.org/10.1029/2003WR002702.

Vaz, C.P., 2003. Use of a Combined Penetrometer-TDR Moisture Probe for Soil Compaction Studies (INIS-XA–989). International Atomic Energy Agency (IAEA).

Van Eerdt, M.M., 1985. Salt marsh cliff stability in the Oosterschelde. Earth Surf. Process. Landforms 10, 95e106.

Wilson, A.M., Morris, J.T., 2012. The influence of tidal forcing on groundwater flow and nutrient exchange in a salt marsh-dominated estuary. Biogeochemistry 108 (1/3), 27–38.

Wilson, A.M., et al., 2015. Groundwater controls ecological zonation of salt marsh macrophytes. Ecology 96 (3), 840–849.

Wilson, C.A., et al., 2012. The effects of crab bioturbation on Mid-Atlantic saltmarsh tidal creek extension: geotechnical and geochemical changes. Estuar. Coast. Shelf Sci. 106, 33–44.

Xin, P., et al., 2010. Soil saturation index of salt marshes subjected to spring-neap tides: a new variable for describing marsh soil aeration condition. Hydrol. Process. 24 (18), 2564–2577. https://doi.org/10.1002/hyp.7670.